Int J Adv Manuf Technol (2014) 75:339–349
DOI 10.1007/s00170-014-6140-9

ORIGINAL ARTICLE

Intelligent measurements for monitoring and control of glass production furnace for green and efficient manufacturing

Tien-I Liu · Carl S. Lyons · S. Sukanya · Che-Hua Yang

Received: 11 May 2014 / Accepted: 1 July 2014 / Published online: 18 July 2014

Abstract Liquefied petroleum (LP) gas is used as one of the fuel systems for glass production furnaces. This research was conducted to develop an intelligent online measurement system for monitoring and control of LP gas so as to achieve green and efficient manufacturing. LP gas is mixed with air at a desired ratio in order to get a proper specific gravity for glass production. Counterpropagation neural networks (CPNs), which are based on competitive learning, were used in this work. Three inputs, air inlet pressure, air/mixed gas differential pressure, and propane/mixed gas differential pressure, were selected for online measurements of specific gravity for monitoring and control of a glass production furnace. Using a 3×12×1 CPN yields exceedingly successful results for online measurements of specific gravity. An average error of 1.68 %, a minimum error of 0.08 %, and a maximum error of 4.43 % were achieved for online measurements. Control actions can then be taken to achieve much higher energy efficiency which is very important for glass production for green and efficient manufacturing.

Keywords Green and efficient manufacturing · CPN · Online measurements

T.-I. Liu (✉) · S. Sukanya
Department of Mechanical Engineering, California State University, Sacramento, CA 95819, USA
e-mail: liut@csus.edu

T.-I. Liu · C.-H. Yang
College of Mechanical and Electrical Engineering, National Taipei University of Technology, Taipei, Taiwan

C. S. Lyons
Cimarron Gas Systems, Inc., Carmichael, CA, USA

1 Introduction

Liquefied petroleum (LP) gas is one kind of fuel used in glass production furnaces. Air is blended with propane vapor in a desired ratio by mixing process to obtain the proper heating value. The compressible gas flow system that is used in the gas blending process of the glass production furnace is highly nonlinear in nature. Variables, including orifices and compressible flow coefficients, make the analysis of the process extremely difficult.

Mixer control system is required to regulate the heating value of the propane and air mixture. The mixture control system is accomplished by sampling the mixed gas from the process. The specific gravity of the mixed gas is then measured, which is proportional to the heating value of the gas. In the glass industry, specific gravity is defined as the ratio of the gas density to the density of air.

The specific gravity is measured by a gravitometer that sends an output signal to the control system for the adjustment of the specific gravity. The control system supervises the position of a series of flow and pressure control valves. The control valves, in turn, regulate the relative amounts of air and propane flowing into a common mixed gas manifold. The mixed gas is then available for glass production furnaces.

This research aims to analyze LP gas as a clean fuel supply for glass production furnaces via online measurements in order to achieve efficient manufacturing [1–6]. This is also very important in achieving green manufacturing for the glass industry since the applications of LP gas technologies can achieve significant carbon savings [7–9].

The specific gravity of the mixed gas stream depends upon the ratio of propane and air flow in the control system. The values of propane/mixed gas differential pressure, air/mixed gas differential pressure, and air inlet pressure into the final control valve affect the specific gravity of the mixed gas [2–4]. These three pressure values were used as inputs for the CPN

and the output is the specific gravity. In this manner, the specific gravity can be estimated by the CPN accurately online to enhance energy efficiency of a glass production furnace without any prior knowledge of the process. This is a novel approach for online measurements of the specific gravity for the control of glass production furnaces.

2 Experimentation

The propane/air mixing system is designed to supply fuel gas to a glass production furnace. The system shown in Fig. 1 consists of a modulating proportional mixer, which regulates mixed gas specific gravity and pressure. The mixer operation requires a continuous supply of propane gas and dry compressed air for operation.

The mixer operation requires propane gas and a clean, dry, compressed air supply for the glass production furnace. Compressed air flows through a control system, from a check valve. Then air is introduced to a sensing and pneumatic control system. From the check valve, the air stream flows through a modulating control valve. This valve adjusts air flow linearly in proportion to its actuator stem position. By modulating the valve position, the relative proportion of air mixing with propane is regulated. Next, the air is introduced to the mixed gas pressure control valve before it enters the mixing manifold vanes. This pressure control valve is coupled to its propane control valve counterpart.

A control valve is used for controlling the mixed gas pressure level. Finally, air flows out of the final control valve and is mixed with propane stream via a series of turbulence vanes. Using this flow sequence, the air pressure level and air proportion are regulated for satisfactory gas blending.

Propane gas is regulated and controlled differently compared to the air flow. The propane is supplied to the mixed gas control valve while maintaining relatively constant pressure. Propane gas is delivered to a pressure regulator for pressure control. The propane enters the mixed gas pressure control valve after it has flowed through the pressure regulator. This valve position depends on the differential pressure between the preceding piping and the mixed gas manifold. Only changes in the mixed gas pressure which occur downstream of the mixed gas control valve affect the differential pressure across this valve because the regulated propane gas pressure is constant.

3 Feature selection

The propane/mix differential pressure, air/mix differential pressure, and air inlet pressure into the final control valve affect the specific gravity of the mixed gas. These three parameters determine the process change. The specific gravity of the mixed gas stream depends upon the ratio of propane/air flow. Since the specific gravity depends upon the flow of the two different compressible gases, the theory of control valve flow is utilized [2–4]. The important flow parameters for the analysis of compressible control valve flow are listed in the following:

- P_1 Upstream absolute pressure (psia)
- P_2 Downstream absolute pressure (psia)
- _P $(P_1–P_2)$, pressure drop
- X $\_P/P_1$, pressure drop ratio
- X_t Terminal pressure drop ratio
- Y $[1 – (X/3X_t)]$ expansion factor
- Q Volumetric flow rate (standard cubic feet per hour)
- F_p Piping geometry factor
- C_v Valve flow coefficient for incompressible fluids
- G Specific gravity of gas, ρ_{gas}/ρ_{air}
- T_t Inlet temperature (°R)
- Z Gas compressibility factor

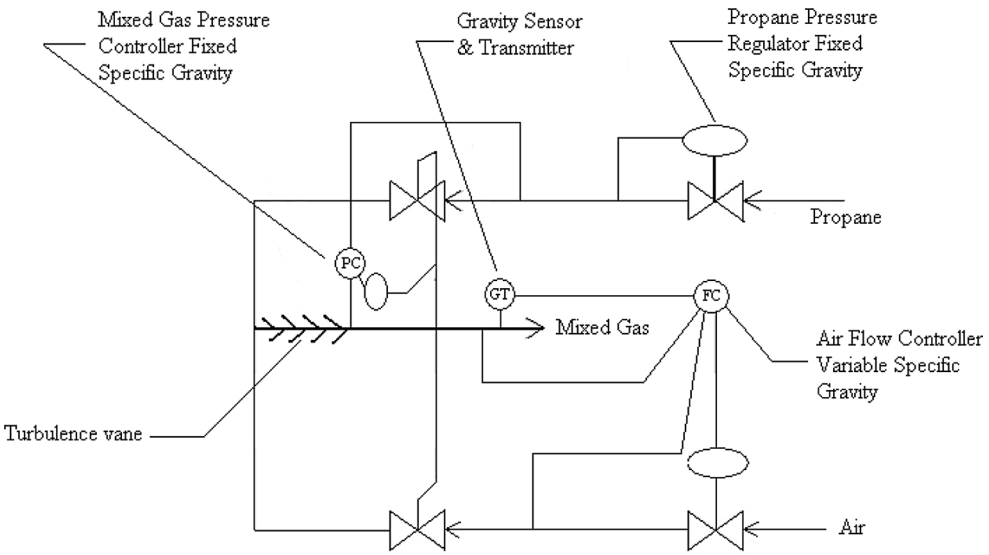

Fig. 1 Propane/air mixer for glass production furnace

For compressible flow through a control valve, the volumetric flow for pressure ratios below the critical pressure ratio, X_t, is defined by Eq. (1). As for the propane/air blending process, the flow parameters that remain constant are F_p, $_G$, T_1, and z, while variable parameters include C_v, P_1, X, and Y.

$$Q = 1,360\, F_p C_v P_1 Y \sqrt{\frac{X}{GT_1 z}} \quad \text{for } X > X_t \tag{1}$$

Flow coefficient, C_v, varies depending upon valve type, size, and area of flow opening [2–4, 10–12]. The C_v parameter varies with flow since it changes with valve position; it is not used as the input of CPN. The factor Y allows correction of C_v value for compressible flow. The expansion factor, Y, cannot be directly measured. By substituting pressure conditions as the input, the expansion factor is taken into account. Pressure drop ratio, X, is measured by sensing differential pressure drop and the inlet pressure [13–15]. Since CPN has the capability to adapt to conditions of incomplete information, the omission of the flow coefficient, C_v, as network input is justified. Therefore, the propane/mix differential pressure, air/mix differential pressure, and air inlet pressure into the final control valve become the three parameters that are extracted from the process and are used as CPN inputs.

4 Artificial neural networks

The objective of this research is to develop an efficient mixing process for the glass production furnace by the use of artificial neural networks [16–21]. Compressible gas flow is nonlinear in nature and involves several different parameters. In addition, variable area orifices compressible flow coefficients make theoretical analysis extremely difficult. Due to the inherent nature of artificial neural network processing, the difficulties of flow modeling can be overcome, and the estimation of specific gravity is made possible.

4.1 Counterpropagation neural networks

Counterpropagation neural network (CPN) is one of the most important artificial neural networks, which is based on competitive learning. It is developed by Hecht Nielsen [22, 23]. Research has been carried out to apply CPNs for statistical analysis, function approximation, online measurements, monitoring, and diagnosis [24–30]. The CPN architecture, illustrated in Fig. 2, consists of three layers as follows: input layer, Kohonen layer, and Grossberg layer.

All of the Kohonen neural neurons are connected to both the input layer and the Grossberg output layer. The connections employ adjustable memory weights that are modified only at the time of network training. Supervised learning requires a training output vector to be presented to the Grossberg layer for error calculation and a training input vector to present information to the Kohonen layer for neural network processing.

Distance tables are formulated in a way that permits each neuron to be chosen on an unbiased basis. The input layer distributes information to the hidden Kohonen neurons for Euclidean distance calculation. From this calculation, the minimum distance is recognized as being the winning neuron. This neuron activation state is excited and is assigned an output value of 1 while the other neuron states are inhibited and the output values are set to be 0. This distance comparison process determines the winning neuron and losing neurons.

After a winning neuron is chosen, the activation output of 1 is passed on to the Grossberg layer. The Grossberg layer receives the activated neuron output of 1 from the Kohonen neuron winner and then computes an output. This output is based on multiplying the Grossberg weights and Kohonen output value of 1. Therefore, the CPN output is the weight of the Grossberg neuron corresponding to the excited memory weight of Kohonen neuron. By the use of an interpolation feature, more than one Kohonen neuron may be excited in order to produce a more accurate neural network output. This is achieved by proportioning the Kohonen neurons output according to their relative closeness and relating this closeness to the sum of their weighted inputs into the Grossberg layer. The counterpropagation neural network parameters are shown as follows:

N	Number of Kohonen neuron
n	Number of input neuron
m	Number of output neuron
X	Input vector of Kohonen layer
Y	Training vector of the Grossberg layer
Z	Output vector of Kohonen layer
Y^*	Output vector of Grossberg layer
W_i	Weight vector of the ith Kohonen neuron
U_j	Weight vector of the jth Grossberg neuron
b_i	Bias for the ith Kohonen neuron
p_i	Win frequency for the ith Kohonen neuron

Determination of the measure of closeness is initialized by computing Euclidean distance between input vector, X, and Kohonen weight vectors, W, as shown in Eq. (2). The resulting distance, d_i, is computed for all the Kohonen neurons. After all the distances have been calculated, the minimum distance can be determined. For training, the winner-take-all algorithm is used. This algorithm is based on the principle that only one neuron provides the output for a given input. The minimum distance is used to activate the neuron associated with that distance. The activation state, Z_i, of the Kohonen layer is then used for the Grossberg weight update.

Euclidean distance between the input vector and Kohonen weight vector W_i is as follows:

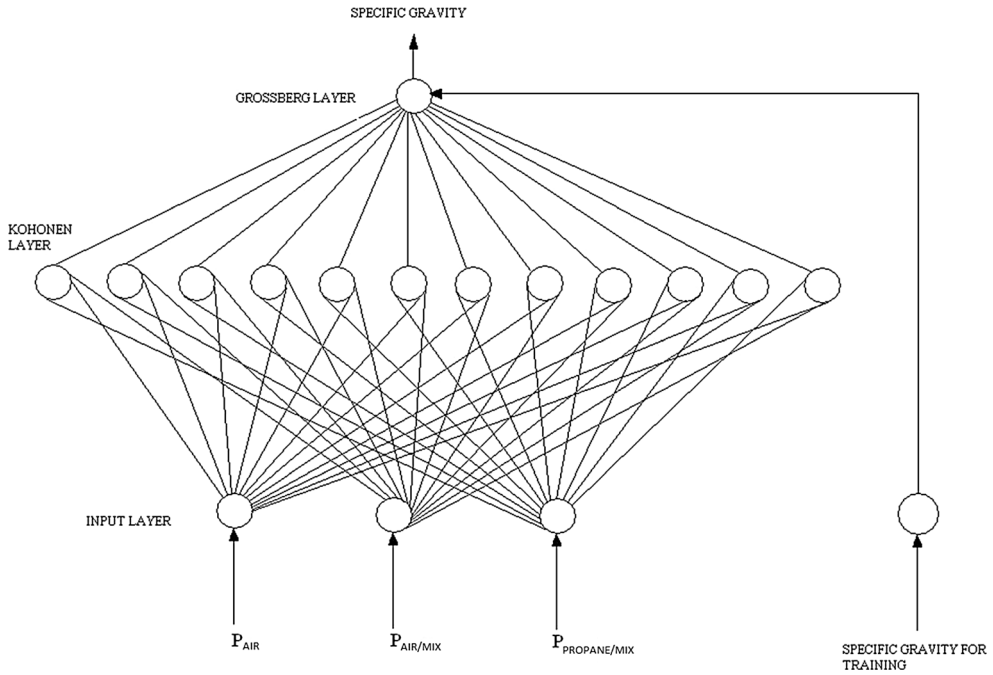

Fig. 2 3×12×1 CPN architecture

$$d_i = \|W_i - X\| = \sqrt{\sum_{j=1}^{n} (W_{ij} - X_j)2} \tag{2}$$

After this, the conscience mechanism feature is used to increase fairness. Since the initial weight values of every Kohonen neuron is selected randomly, the probability of every neuron to win for learning is not equal. Some of Kohonen neurons will win much more frequently than others. Therefore, a bias distance b_i, as shown in Eq. (3), is used to increase the probability of those neurons which lose too often by drawing them to the training regions.

The frequent winning punishment to increase fairness is shown as follows:

$$\begin{aligned} d_i' &= d_i && \text{if win frequency } p_i < T \\ d_i' &= (d_i - b_i) && \text{if win frequency } p_i \geq T \\ T &= 1/(15N) && \text{(threshold win frequency)} \end{aligned} \tag{3}$$

The selection of the winner after frequent winning punishment has been implemented as follows:

$$\begin{aligned} Z_i' &= 1 && \text{for index i which corresponds to } d_i' \leq d_j' \\ Z_i' &= 0 && \text{for all other cases} \end{aligned} \tag{4}$$

No penalties are assessed to neurons that remain inactive much of the time. Neurons that win too frequently are inactivated by putting a bias distance to their Euclidean distance. This allows other neurons that previously held longer Euclidean distances to win more often. The threshold win frequency T, presented in Eq. (3), must be exceeded by a neuron winning probability in order for the bias distance feature to be implemented.

In order to enhance CPN training, an interpolation mechanism is added to the neural network. Interpolation allows the neural network output to be proportionally shared, on the Grossberg layer, by more than one Kohonen neuron. By selecting the Kohonen neurons closest in distance to the input vector, and proportioning each neuron accordingly, the neural network training can be further enhanced as described in Eqs. (5)–(7).

$$\begin{aligned} d_j &= \text{Euclidean distance of neurons considered} \\ d_0 &= \min(d_i) \\ e_i &= d_0/d_i \\ &= 1 \qquad \text{if } d_i = d_0 \end{aligned} \tag{5}$$

$$f_i = e_i^r \qquad r = 1.0 \text{ typically} \tag{6}$$

Kohonen layer output of neuron i is

$$Z_i = f_i / \sum_{j=1}^{N} f_j \tag{7}$$

4.2 Counterpropagation network training

Counterpropagation neural networks are trained in two stages. In the first stage, the Kohonen neuron weights are adjusted to match the input. After this, the second training stage helps to adjust the Grossberg weights in order to fit the desired neuron output.

Table 1 Training data sets

Data Number	Air inlet pressure kg/cm^2 (psi)	Air/mix pressure kg/cm^2 (psi)	Propane/mix pressure kg/cm^2 (psi)	Mix specific gravity
1	2.102269 (29.9)	0.014062 (0.2)	0.140620 (2.0)	1.19
2	2.123362 (30.2)	0 (0)	0.140620 (2.0)	1.20
3	2.102269 (29.9)	0.014062 (0.2)	0.140620 (2.0)	1.22
4	2.643656 (37.6)	0.063279 (0.9)	0 (0)	1.22
5	2.453819 (34.9)	0.154682 (2.2)	0.112496 (1.6)	1.22
6	2.137424 (30.4)	0.014062 (0.2)	0.098434 (1.4)	1.22
7	2.256951 (32.1)	0.028124 (0.4)	0.112496 (1.6)	1.22
8	2.720997 (38.7)	0.140620 (2.0)	0.007031 (0.1)	1.23
9	2.390540 (34.0)	0.161713 (2.3)	0.175775 (2.5)	1.23
10	2.123362 (30.2)	0.035155 (0.5)	0.161713 (2.3)	1.23
11	2.313199 (32.9)	0.014062 (0.2)	0.147651 (2.1)	1.23
12	2.320230 (33.0)	0.056248 (0.8)	0.126558 (1.8)	1.24
13	2.235858 (31.8)	0.007031 (0.1)	0.133589 (1.9)	1.25
14	2.172579 (30.9)	0.014062 (0.2)	0.105465 (1.5)	1.25
15	2.158517 (30.7)	0.035155 (0.5)	0.133589 (1.9)	1.25
16	2.784276 (39.6)	0.168744 (2.4)	0.007031 (0.1)	1.25
17	2.460850 (35.0)	0.021093 (0.3)	0.091403 (1.3)	1.25
18	2.355385 (33.5)	0.056248 (0.8)	0 (0)	1.26
19	2.341323 (33.3)	0.042186 (0.6)	0.133589 (1.9)	1.26
20	2.046021 (29.1)	0.028124 (0.4)	0.182806 (2.6)	1.26
21	2.200703 (31.3)	0.077341 (1.1)	0.140620 (2.0)	1.27
22	2.242889 (31.9)	0.084372 (1.2)	0.147651 (2.1)	1.27
23	2.109300 (30.0)	0.021093 (0.3)	0.147651 (2.1)	1.27
24	2.172579 (30.9)	0.014062 (0.2)	0.140620 (2.0)	1.27
25	2.144455 (30.5)	0.056248 (0.8)	0.133589 (1.9)	1.27
26	3.002237 (42.7)	0.386705 (5.5)	0.07031 (1.0)	1.27
27	2.207734 (31.4)	0.084372 (1.2)	0.14062 (2.0)	1.28
28	3.072547 (43.7)	0.421860 (6.0)	0.014062 (0.2)	1.28
29	2.193672 (31.2)	0.070310 (1.0)	0.133589 (1.9)	1.28
30	3.121764 (44.4)	0.471077 (6.7)	0 (0)	1.28
31	2.228827 (31.7)	0.14062 (2.0)	0.154682 (2.2)	1.28
32	2.228827 (31.7)	0.14062 (2.0)	0.14062 (2.0)	1.28
33	2.306168 (32.8)	0.147651 (2.1)	0.224992 (3.2)	1.28
34	2.249920 (32.0)	0.126558 (1.8)	0.140620 (2.0)	1.28
35	2.165548 (30.8)	0.077341 (1.1)	0.140620 (2.0)	1.28
36	2.228827 (31.7)	0.070310 (1.0)	0.105465 (1.5)	1.29
37	2.172579 (30.9)	0.049217 (0.7)	0.084372 (1.2)	1.29
38	2.221796 (31.6)	0.063279 (0.9)	0.126558 (1.8)	1.29
39	2.242889 (31.9)	0.084372 (1.2)	0.105465 (1.5)	1.29
40	2.172579 (30.9)	0.084372 (1.2)	0.154682 (2.2)	1.29
41	2.228827 (31.7)	0.070310 (1.0)	0.070310 (1.0)	1.29
42	2.299137 (32.7)	0.140620 (2.0)	0.175775 (2.5)	1.30
43	2.172579 (30.9)	0.084372 (1.2)	0.147651 (2.1)	1.30
44	2.299137 (32.7)	0.140620 (2.0)	0.126558 (1.8)	1.30
45	2.263982 (32.2)	0.140620 (2.0)	0.070310 (1.0)	1.30
46	2.158517 (30.7)	0.070310 (1.0)	0.126558 (1.8)	1.31
47	2.306168 (32.8)	0.147651 (2.1)	0.084372 (1.2)	1.32
48	2.158517 (30.7)	0.070310 (1.0)	0.140620 (2.0)	1.32
49	2.369447 (33.7)	0.070310 (1.0)	0.084372 (1.2)	1.32

Table 1 (continued)

Data Number	Air inlet pressure kg/cm^2 (psi)	Air/mix pressure kg/cm^2 (psi)	Propane/mix pressure kg/cm^2 (psi)	Mix specific gravity
50	2.369447 (33.7)	0.210930 (3.0)	0.154682 (2.2)	1.33
51	2.334292 (33.2)	0.175775 (2.5)	0.140620 (2.0)	1.33
52	2.263982 (32.2)	0.140620 (2.0)	0.168744 (2.4)	1.33
53	2.285075 (32.5)	0.140620 (2.0)	0.154682 (2.2)	1.34
54	2.228827 (31.7)	0.105465 (1.5)	0.112496 (1.6)	1.35
55	2.249920 (32.0)	0.091403 (1.3)	0.140620 (2.0)	1.37
56	2.334292 (33.2)	0.210930 (3.0)	0.112496 (1.6)	1.37
57	2.383509 (33.9)	0.260147 (3.7)	0.140620 (2.0)	1.38
58	2.404602 (34.2)	0.175775 (2.5)	0.112496 (1.6)	1.38
59	2.474912 (35.2)	0.316395 (4.5)	0.084372 (1.2)	1.38
60	2.383509 (33.9)	0.260147 (3.7)	0.140620 (2.0)	1.39
61	2.355385 (33.5)	0.267178 (3.8)	0.133589 (1.9)	1.41
62	2.362416 (33.6)	0.274209 (3.9)	0.140620 (2.0)	1.41
63	2.404602 (34.2)	0.246085 (3.5)	0.140620 (2.0)	1.42

By measuring the distance between the Kohonen neuron weight vectors and the input weight vectors, CPN learning begins. The calculated distances are compared and a minimum distance is used to identify the winning neuron. The victorious neuron weight vector is moved slightly closer to the input training vector while the other neuron weights are left unchanged. This process of moving clusters of Kohonen weight vector closer toward the input vector is repeated. However, the weight clusters may become unfairly biased in their weight update frequency. Therefore, a "conscience" mechanism is used to circumvent this update inclination [22, 27, 31]. If each Kohonen neuron is chosen without bias, the winning neuron probability would be the reciprocal of the number of neurons involved. Due to the random nature of the starting weight selection for the Kohonen neurons, the probability that the neurons will be chosen for weight adaptation is not the same for all the neurons. Therefore, some of the neurons will be frequently adjusting their weights while the weights of some other neurons may become static.

The difference between the target win frequency, 1/N, and the computed win frequency, p_i, is used as a measure of error probability. This probability error, multiplied by an error factor, c, is higher during the initial stages of training and decreases as training takes place. The factor c is a function of the number of Kohonen neurons, N, and the number of inputs, n, as seen in Eq. (9). The recommended value for c should be decreased over time because the Kohonen neurons will be moving closer to their unbiased weight spaces.

Bias distance is

$$b_i = c\,(1/N - p_i) \tag{8}$$

Probability error factor is

$$c = N\sqrt{n}/8 \tag{9}$$

The computed win frequency, p_i, is a function of the neuron output state, Z_i', the previous win probability, p_i, and

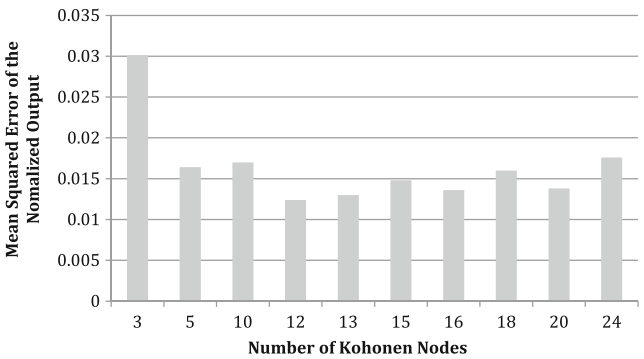

Fig. 3 Mean squared errors versus number of Kohonen neurons

Table 2 Output error of various CPN architectures

Architecture	Mean squared error of normalized output
3×3×1	0.0301
3×5×1	0.0164
3×10×1	0.0170
3×12×1	0.0124
3×13×1	0.0130
3×15×1	0.0148
3×16×1	0.0136
3×18×1	0.0160
3×20×1	0.0138
3×24×1	0.0176

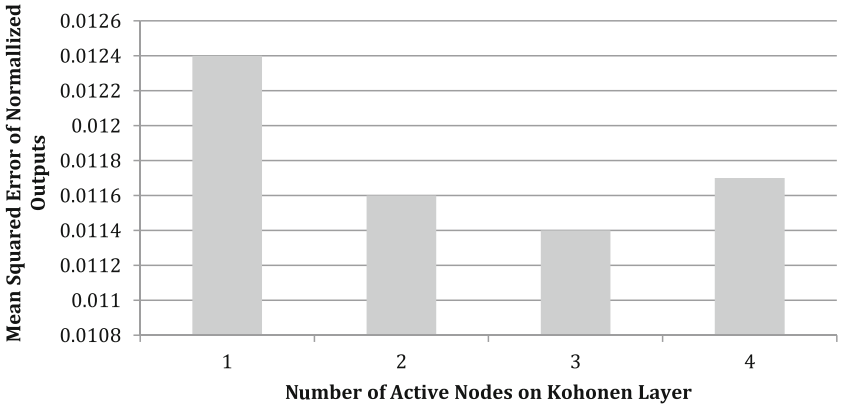

Fig. 4 Mean squared errors versus number of active Kohonen nodes for a 3×12×1 CPN

probability error factor, b. The relation is defined in Eq. (10). The appropriate value of probability error factor, b, is given by Eq. (11).

Win frequency is

$$p_i^{new} = p_i^{old} + b\left(Z_i' - p_i^{old}\right) \tag{10}$$

Probability error factor is

$$b = (1/10)N \tag{11}$$

The weight vector update rule is dependent upon the previous weight, W_i^{old}, Kohonen learning rate, the input vector, X, and the output of the Kohonen layer, z_i', as indicated by Eq. (12). A suggested, initial learning rate is 0.02 and then decreased over time.

Kohonen weight update rule is shown in Eq. (12) as follows:

$$W_i^{new} = W_i^{old} + A\left(X - W_i^{old}\right)Z_i' \tag{12}$$

Finally, the output from the Kohonen layer is presented to the Grossberg layer for additional tuning. The weight parameter relationship is described in Eq. (13). The difference between the training value, Y_k, and the Grossberg weight, U_{ki}, is computed for each neuron weight connection. This weight difference is modified by error factor, a, and combined with the previous neuron weight. Grossberg weights that are not aligned with an activated Kohonen neuron remain unchanged. Grossberg neuron output is defined as the product of the Grossberg weights, U_{ki}, and Kohonen output, Z_i. CPN training iteration is terminated after the network reaches an acceptable error or residual error.

$$\begin{aligned} &\text{If } Z_i = 1, \quad U_{ki}^{new} = U_{ki}^{old} + a\left(Y_k - U_{ki}^{old}\right) \\ &\text{If } Z_i = 0, \quad U_{ki}^{new} = U_{ki}^{old} \end{aligned} \tag{13}$$

A suggested, Grossberg learning rate a is 0.3 and is reduced over time. The Grossberg neuron output is

$$Y'_k = U_k Z = \sum_{i=1}^{N} U_{ki} Z_i \tag{14}$$

Table 3 3×12×1 counterpropagation neural network interpolation number versus error

Number of Kohonen neuron interpolations	Mean squared error of normalized output
1	0.0124
2	0.0116
3	0.0114
4	0.0117

Table 4 Final weights of 3×12×1 CPN

Neuron number on the Kohonen layer	Input neuron			Grossberg layer weights
	1	2	3	
1	0.277	0.125	0.563	0.248
2	0.287	0.188	0.519	0.376
3	0.247	0.181	0.615	0.340
4	0.556	0.274	0.110	0.268
5	0.415	0.522	0.556	0.779
6	0.207	0.157	0.263	0.000
7	0.361	0.333	0.488	0.485
8	0.725	0.747	0.281	0.391
9	0.365	0.359	0.669	0.462
10	0.326	0.223	0.566	0.426
11	0.372	0.230	0.416	0.434
12	0.267	0.136	0.395	0.286

Table 5 On-line test data

Data number	Air inlet pressure kg/cm^2 (psi)	Air/mix pressure kg/cm^2 (psi)	Propane/mix pressure kg/cm^2 (psi)	Mix specific gravity
1	2.165548 (30.8)	0.007031 (0.1)	0.091403 (1.3)	1.22
2	2.664749 (37.9)	0.014062 (0.2)	0.014062 (0.2)	1.23
3	2.728028 (38.8)	0.042186 (0.6)	0.007031 (0.1)	1.23
4	2.657718 (37.8)	0.077341 (1.1)	0 (0)	1.23
5	2.200703 (31.3)	0.007031 (0.1)	0.091403 (1.3)	1.24
6	2.777245 (39.5)	0.126558 (1.8)	0.007031 (0.1)	1.24
7	2.376478 (33.8)	0.007031 (0.1)	0.133589 (1.9)	1.24
8	2.067114 (29.4)	0 (0)	0.091403 (1.3)	1.25
9	2.123362 (30.2)	0.035155 (0.5)	0.126558 (1.8)	1.25
10	2.362416 (33.6)	0.063279 (0.9)	0.140620 (2.0)	1.25
11	2.861617 (40.7)	0.210930 (3.0)	0.014062 (0.2)	1.25
12	2.186641 (31.1)	0.098434 (1.4)	0.154682 (2.2)	1.25
13	2.137424 (30.4)	0.014062 (0.2)	0.147651 (2.1)	1.25
14	2.524129 (35.9)	0.154682 (2.2)	0.084372 (1.2)	1.25
15	2.306168 (32.8)	0.007031 (0.1)	0.133589 (1.9)	1.25
16	2.974113 (42.3)	0.323426 (4.6)	0.014062 (0.2)	1.26
17	1.982742 (28.2)	0.035155 (0.5)	0.147651 (2.1)	1.26
18	2.510067 (35.7)	0 (0)	0.105465 (1.5)	1.26
19	2.960051 (42.1)	0.379674 (5.4)	0.084372 (1.2)	1.27
20	2.207734 (31.4)	0.084372 (1.2)	0.140620 (2.0)	1.27
21	2.060083 (29.3)	0.042186 (0.6)	0.196868 (2.8)	1.27
22	2.186641 (31.1)	0.028124 (0.4)	0.105465 (1.5)	1.27
23	2.404602 (34.2)	0.105465 (1.5)	0.084372 (1.2)	1.27
24	2.334292 (33.2)	0 (0)	0.084372 (1.2)	1.27
25	2.404602 (34.2)	0.105465 (1.5)	0.091403 (1.3)	1.27
26	2.172579 (30.9)	0.014062 (0.2)	0.105465 (1.5)	1.27
27	2.235858 (31.8)	0.077341 (1.1)	0.126558 (1.8)	1.28
28	2.650687 (37.7)	0.210930 (3.0)	0.063279 (0.9)	1.28
29	2.200703 (31.3)	0.077341 (1.1)	0.133589 (1.9)	1.28
30	2.207734 (31.4)	0.084372 (1.2)	0.126558 (1.8)	1.28
31	2.193672 (31.2)	0.070310 (1.0)	0.140620 (2.0)	1.28
32	2.193672 (31.2)	0.070310 (1.0)	0.126558 (1.8)	1.28
33	3.009268 (42.8)	0.358581 (5.1)	0.014062 (0.2)	1.28
34	2.228827 (31.7)	0.070310 (1.0)	0.091403 (1.3)	1.28
35	2.271013 (32.3)	0.182806 (2.6)	0.140620 (2.0)	1.28
36	2.200703 (31.3)	0.077341 (1.1)	0.140620 (2.0)	1.28
37	2.228827 (31.7)	0.140620 (2.0)	0.126558 (1.8)	1.28
38	2.221796 (31.6)	0.133589 (1.9)	0.126558 (1.8)	1.28
39	2.172579 (30.9)	0.084372 (1.2)	0.140620 (2.0)	1.29
40	2.608501 (37.1)	0.168744 (2.4)	0.084372 (1.2)	1.29
41	2.320230 (33.0)	0.161713 (2.3)	0.084372 (1.2)	1.29
42	2.207734 (31.4)	0.084372 (1.2)	0.147651 (2.1)	1.29
43	2.263982 (32.2)	0.070310 (1.0)	0.091403 (1.3)	1.29
44	2.299137 (32.7)	0.140620 (2.0)	0.126558 (1.8)	1.29
45	2.130393 (30.3)	0.077341 (1.1)	0.147651 (2.1)	1.30
46	2.228827 (31.7)	0.070310 (1.0)	0.098434 (1.4)	1.30
47	2.256951 (32.1)	0.133589 (1.9)	0.112496 (1.6)	1.30
48	2.249920 (32.0)	0.126558 (1.8)	0.133589 (1.9)	1.30
49	2.285075 (32.5)	0.126558 (1.8)	0.140620 (2.0)	1.31

Table 5 (continued)

Data number	Air inlet pressure kg/cm^2 (psi)	Air/mix pressure kg/cm^2 (psi)	Propane/mix pressure kg/cm^2 (psi)	Mix specific gravity
50	2.158517 (30.7)	0 (0)	0.140620 (2.0)	1.31
51	2.341323 (33.3)	0.147651 (2.1)	0.105465 (1.5)	1.32
52	2.263982 (32.2)	0.105465 (1.5)	0.112496 (1.6)	1.32
53	2.362416 (33.6)	0.239054 (3.4)	0.126558 (1.8)	1.33
54	2.285075 (32.5)	0.126558 (1.8)	0.140620 (2.0)	1.33
55	2.425695 (34.5)	0.232023 (3.3)	0.105465 (1.5)	1.37
56	2.355385 (33.5)	0.267178 (3.8)	0.140620 (2.0)	1.38
57	2.439757 (34.7)	0.281240 (4.0)	0.098434 (1.4)	1.38
58	2.432726 (34.6)	0.274209 (3.9)	0.098434 (1.4)	1.38
59	2.369447 (33.7)	0.175775 (2.5)	0.140620 (2.0)	1.38
60	2.411633 (34.3)	0.182806 (2.6)	0.098434 (1.4)	1.39
61	2.411633 (34.3)	0.217961 (3.1)	0.105465 (1.5)	1.40
62	2.418664 (34.4)	0.224992 (3.2)	0.126558 (1.8)	1.41
63	2.369447 (33.7)	0.281240 (4.0)	0.140620 (2.0)	1.42

5 Online measurements for monitoring and control of glass production furnace

For online measurements of the specific gravity of the LP gas for monitoring and control of glass production furnace, three features were used as the inputs. These three features are the air inlet pressure, the propane/mixed gas differential pressure, and the air/mixed gas differential pressure.

The measured values of these three features were used as inputs of counterpropagation neural networks (CPNs). Specific gravity can be estimated online by the CPNs. The pressure values were used as indirect indices for the online measurements of the specific gravity. This intelligent system can be operated on the real-time basis. Therefore, it can predict specific gravity so as to take control actions to achieve energy efficiency. Furthermore, this system can predict specific gravity before it may exceed its limits. Instead of complete shutting down the mixer in case of extreme conditions, corrective actions can be taken in advance before the process gets out of control. Diagnostic actions, allowed by this intelligent system, can prevent undesirable catastrophic shut down of glass production furnace, which greatly enhance the process reliability.

5.1 Training process of counterpropagation neural networks

Sixty-three sets of data were presented to the counterpropagation neural networks for the purpose of learning. The training sets are shown in Table 1. Data were normalized from 0.1 to 0.9 before being presented to the neural networks. Ten different CPN architectures with different number of Kohonen neurons were used.

The comparison of the mean squared error of the normalized output for various CPN architectures is shown in Fig. 3 and Table 2. The mean squared error of the normalized output ranges from 0.0124 to 0.0301. The 3×12×1 CPN architecture was selected since it has the smallest mean squared error with a value of 0.0124.

The performance of the 3×12×1 CPN with interpolation was then compared with the same network architecture without using the interpolation. The interpolation feature uses a proportional relationship to calculate Grossberg output for more than one of the Kohonen nodes that was measured to be closest to the input set in order to further enhance the performance of CPN. Up to four Kohonen nodes were used, as illustrated in Fig. 4 and Table 3. The mean squared error of the normalized output ranges from 0.0114 to 0.0124. The best performance was achieved by the 3×12×1 counterpropagation neural network with an interpolation of three Kohonen nodes in closest proximity to the input set, which further reduced the mean squared error to be 0.0114. Therefore, it was chosen for online tests.

During the training process, the Kohonen layer learning rate, $A=0.02$, and the Grossberg layer learning rate, $a=0.3$, are defined. Probability error factor, b, is assigned a value of 0.0083 and the bias threshold barrier, T, is given a value of 0.0056. The training of counterpropagation neural networks, being two-stage in nature, requires that the hidden Kohonen layer be trained first. The Kohonen layer learning rate is gradually reduced from $A=0.02$ to $A=0.001$ overtime until it ceases to adjust its weights any further. At this time, the learning of the Grossberg layer may begin. The Grossberg learning rate starting value of $a=0.3$ was reduced to $a=0.05$ after 2,000 iterations and finally was reduced to $a=0.01$ after another 4,000 more training iterations. The final weights of the 3×12×1 counterpropagation neural network are shown in Table 4.

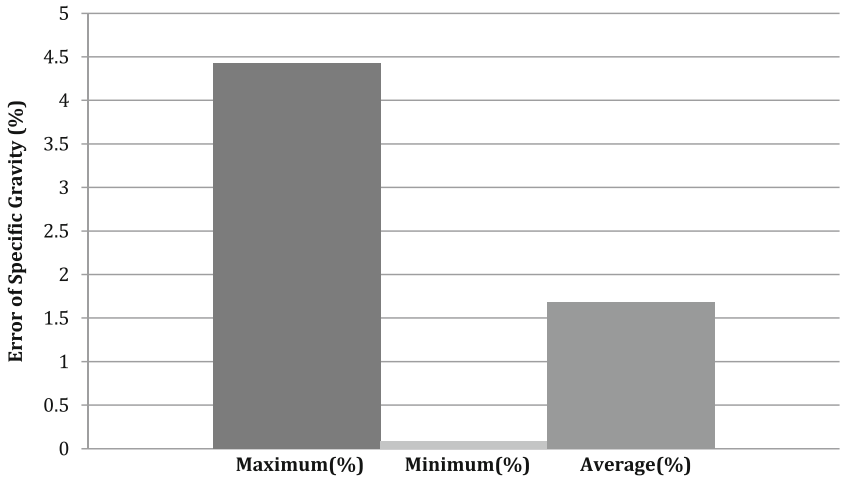

Fig. 5 The estimation error of 3×12×1 CPN

5.2 Online tests using counterpropagation neural networks

Another 63 data sets were used for the online tests. Online test data sets are listed in Table 5.

The 3×12×1 CPN yields excellent results for the online measurements of the specific gravity of the LP gas, as shown in Figs. 5, 6, and Table 6. The percent error ranges from 0.08 to 4.43 % with an error standard deviation of 0.0326. These are very accurate results for online measurements. In other words, using a 3×12×1 counterpropagation neural network, an average error of 1.68 %, a maximum error of 4.43 %, and a minimum error of 0.08 % have been achieved. Therefore, it is selected for the online measurements so as to control the specific gravity of the LP gas for the glass production furnace.

This intelligent system can predict specific gravity before it exceeds predetermined limits. Control actions can be taken in advance before the process gets out of control. Diagnostic actions, allowed by this intelligent system, can prevent undesirable catastrophic shut down of glass production furnaces. Therefore, process reliability can be greatly enhanced. Furthermore, this intelligent system can measure specific gravity online very accurately. This will allow the control system to keep the specific gravity in an adequate level so as to achieve much higher energy efficiency in glass production. This will make manufacturing more efficient and greener.

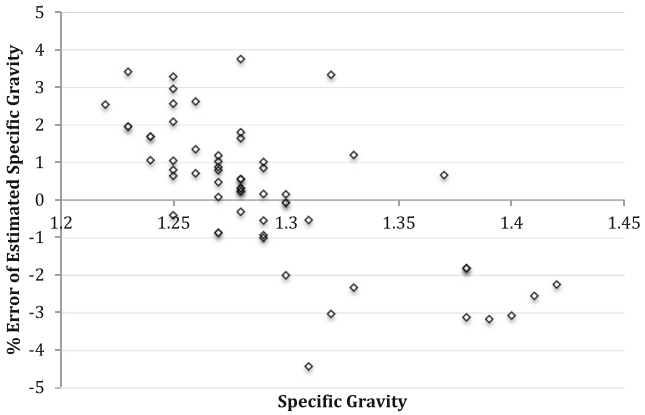

Fig. 6 Errors of measured versus estimated specific gravity of a 3×12×1 CPN

6 Conclusions

The compressible gas flow system that is used in the gas blending process of the glass production furnace is nonlinear in nature. Variables, including orifices and compressible flow coefficients, make the analysis of the process extremely difficult. Counterpropagation neural networks can perform online measurements without any prior knowledge of the process. Based on this research, the following conclusions can be drawn:

1. Three features were selected from the control system of the glass production furnace for online monitoring and diagnosis. These three features are air inlet pressure, propane/mixed gas differential pressure, and air/mixed gas differential pressure. Integrating these three features as the inputs of neural networks generates excellent online specific gravity estimation.
2. A 3×12×1 CPN can accurately measure the specific gravity of the LP gas online with an average error of 1.68 %, a minimum error of 0.08 %, and a maximum error of 4.43 %.
3. The 3×12×1 CPN yields exceedingly successfully results for the online measurements of the specific gravity of the

Table 6 The 3×12×1 CPN output error

CPN Architecture	Error (%)		
	Maximum	Minimum	Average
3×12×1 CPN	4.43	0.08	1.68

LP gas for the glass production furnace. Control actions can be taken to achieve much higher energy efficiency which is very important for glass production for green and efficient manufacturing.

4. This intelligent system can predict specific gravity before it exceeds predetermined limits. Corrective actions can be taken in advance before the process gets out of control. Diagnostic actions, allowed by this intelligent system, can prevent undesirable catastrophic shut down of glass production furnaces. Therefore, process reliability can be greatly enhanced.

Acknowledgment Partial support of this research by Cimarron Gas Systems, Inc. and Gallo Glass Company is greatly appreciated.

References

1. Abu-Zahra NH, Karimi S (2002) On-line monitoring of PVC foam density using ultrasound waves and artificial neural networks. Int J Adv Manuf Technol 19:618–622
2. Glass Manufacturing Industry Council (GMIC) (2000) Workshop Proceedings: Advances in Combustion Technologies for Glass Processing. Pittsburgh, PA
3. Makarov RI, Suvorov E (2010) Increasing the quality of tempered glass on an operating process line. Glas Ceram 67(5):18–21
4. Liu TI, Kumagai A, Lyons C (2006) On-line measurements for monitoring and diagnosis of glass production furnace. J CSME 27(5):587–592
5. Shahsbi HM, Ratnam MM (2009) In-cycle monitoring of tool nose wear and surface roughness of turned parts using machine vision. Int J Adv Manuf Technol 40:1148–1157
6. Sharmr VS, Shama SK, Shama AK (2008) Cutting tool wear estimation for turning. J Intell Manuf 19:99–108
7. Dornfeld DA (2014) Moving toward sustainable and green manufacturing. Int J Precis Eng Manuf-Green Technol 1(1):63–66
8. Ahn SH (2014) An evaluation of green manufacturing technologies based on research databases. Int J Precis Eng Manuf-Green Technol 1(1):5–9
9. The trade association for the LP Gas industry in the UK (2014) Targeting Carbon Reduction in Off Grid Britain. http://www.uklpg.org/exceptional-energy/targeting-carbon-reduction-in-off-grid-britain/
10. Baumann HD (2008) Control valve primer: a user's guide, 4th edition, the instrumentation, systems, and automation society. North Carolina, USA
11. Co C (2013) Flow of fluids through valves, fittings, and pipe. Crane Valve Group, Stamford
12. Fisher Controls International, Emerson Process Management (2005) Control Valve Handbook, 4th edn. Fisher Controls International, Marshalltown
13. Nesbitt B (2007) Handbook of valves and actuators. Butterworth-Heinemann, Oxford
14. Prasad J, Jayaswal MN, Priye V (2011) Instrumentation and Process Control. International Publishing House, I K
15. Skousen PL (2011) Valve Handbook, 3rd edn. McGraw-Hall, New York
16. Baraldi P, Compare M, Sauco S, Zio E (2013) Ensemble neural network-based particle filtering for prognostics. Mech Syst Signal Process 41(1–2):288–300
17. Liu TI, Kumagai A, Wang YC et al (2010) On-line monitoring of boring tools for control of boring operations. Robot Comput Integr Manuf 26:230–239
18. Liu TI, Lee J, Singh P, Liu G (2014) Real-time recognition of ball bearing states for the enhancement of precision, quality, efficiency, safety, and automation of manufacturing. Int J Adv Manuf Technol 71(5):809–816
19. Liu TI, Song SD, Liu G, Wu Z (2013) On-line monitoring and measurements of tool wear for precision turning of stainless steel parts. Int J Adv Manuf Technol 65(9):1397–1407
20. Worden K, Staszewski W, Hensman J (2011) Natural computing for mechanical systems research: a tutorial overview. Mech Syst Signal Process 25:4–111
21. Xie SL, Zhang YH, Chen CH, Zhang XN (2013) Identification of nonlinear hysteretic systems by artificial neural networks. Mech Syst Signal Process 34(1):76–87
22. Russell S, Norvig P (2010) Artificial intelligence: a modern approach. 3rd edition. Prentice Hall, Pearson Education, Inc, New Jersey
23. Vemuri V, Hecht-Nielson R (1988) Artificial neural networks: theoretical concepts. IEEE Computer Society Press, Washington
24. Barakat M, El Badaoui M, Guillet F (2013) Hard competitive growing neural network for the diagnosis of small bearing faults. Mech Syst Signal Process 37(1–2):276–292
25. Gologlu C, Arslan Y (2009) Zigzag machining surface roughness modeling using evolutionary approach. J Intell Manuf 20: 203–210
26. Huang R, Xi L, Li X, Liu CR, Qiu H, Lee J (2007) Residual life predictions for ball bearings based on self-organizing map and back propagation neural network methods. Mech Syst Signal Process 21: 193–207
27. Liu TI, Ordukhani F, Jani D (2005) Monitoring and diagnosis of roller bearing conditions using neural networks and soft computing. Int J Knowl-based and IntellEng Syst 9(2):149–157
28. Raafat SM, Akmeliawati R, Matono W (2010) Intelligent robust control design of a precise positioning system. Int J Control Autom Syst 8(5):1123–1132
29. Samanta B, Nataraj C (2008) Prognostics of machine condition using soft computing. Robot Comput Integr Manuf 24: 816–823
30. Vora N, Tambe SS, Kulkarni BD (1997) Counterpropagation neural networks for fault detection and diagnosis. Comput Chem Eng 21(2): 177–185
31. De Sieno D (1988) Adding a Conscience to Competitive Learning. Proceeding of IEEE International Coference on Neural Networks. IEEE San Diego Section, San Diego, CA, 1: 117–124